Supplementary materials

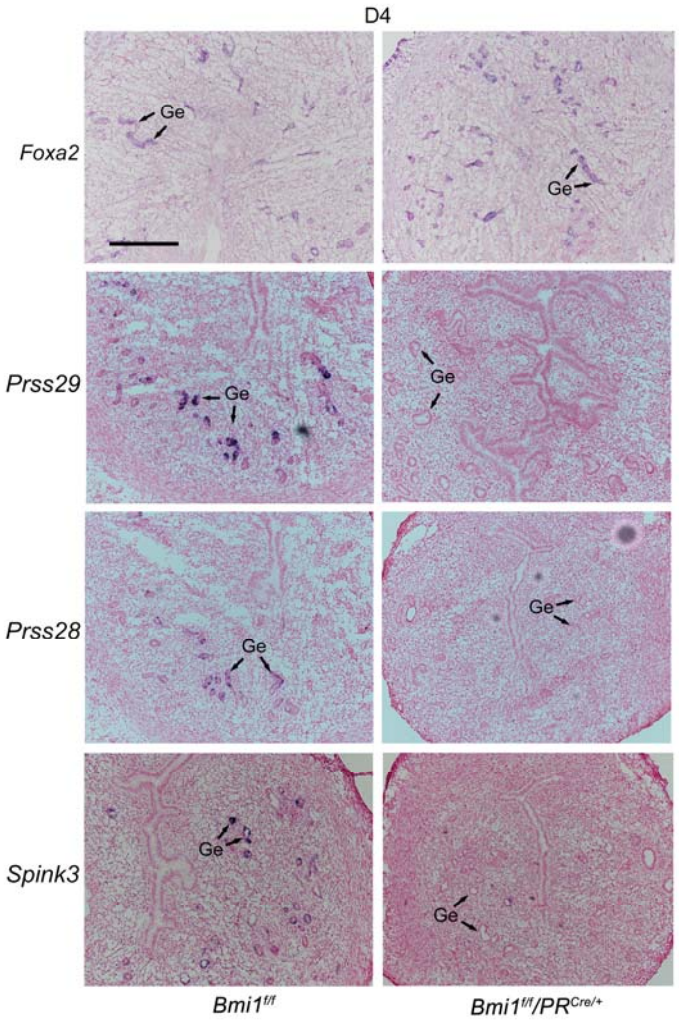

Supplementary Figure 1: The normal expression of uterine gland specific genes is derailed in Bmi1$^{d/d}$ uteri

In situ hybridization with the DIG-labeled probe analysis the gland-specific genes in *Bmi1*$^{f/f}$, *Bmi1*$^{d/d}$ mice. Ge, glandular epithelium. Black scale bar, 100 μm.

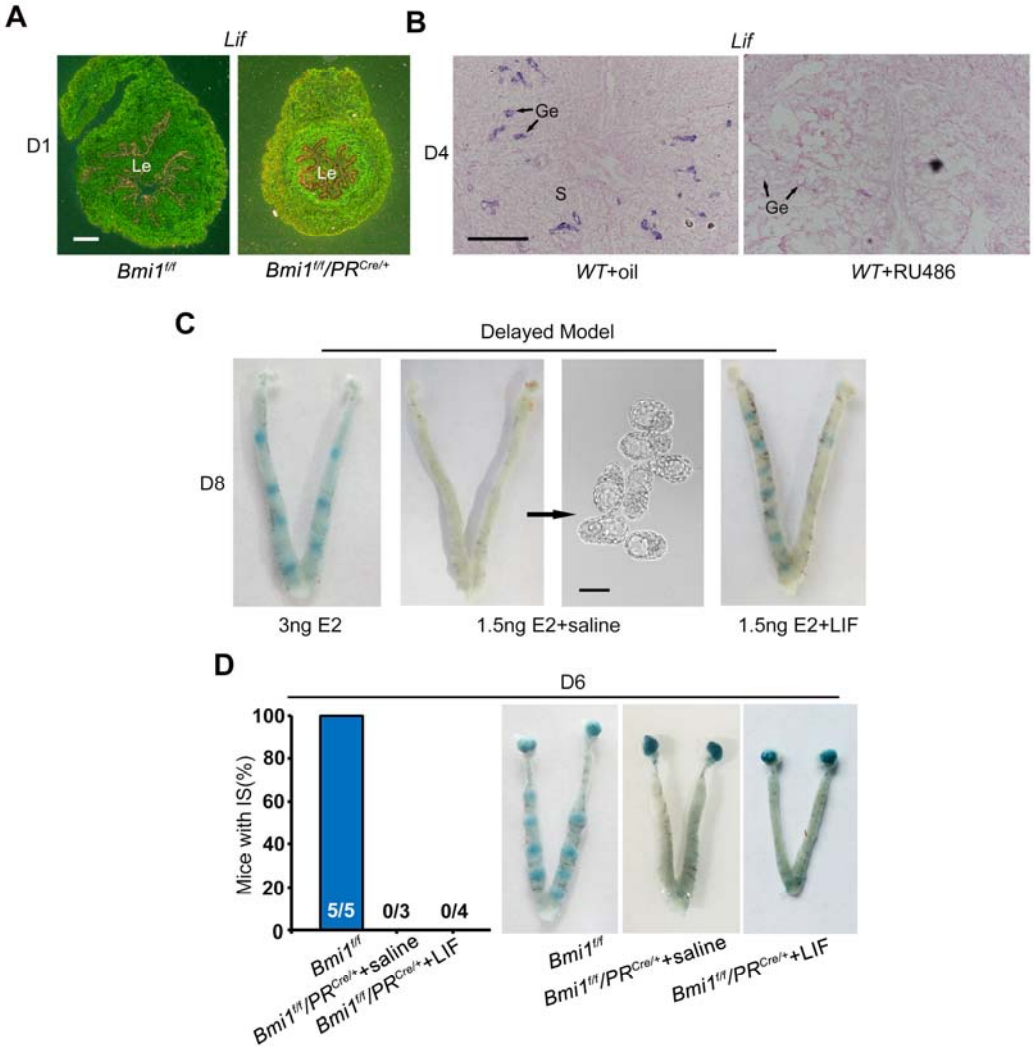

Supplementary Figure 2: Exogenous LIF supplement cannot restore the implantation defect in Bmi1 mutant females

(**A**) *In situ* hybridization analysis indicates a comparable expression level of *Lif* in day 1 *Bmi1*$^{f/f}$ and *Bmi1*$^{d/d}$ uteri. White scale bar, 100 μm; Le, luminal epithelium. (**B**) *In situ* hybridization analysis reveals the PR antagonist RU486 treatment on Day 3 would influence the *Lif* expression on day 4 uterine gland. Ge, glandular epithelium. Black scale bar, 100 μm. (**C**) Representative morphology of uteri from delayed model with different treatments. (**D**) Implantation rate and representative morphology of uteri from *Bmi1*$^{f/f}$, *Bmi1*$^{d/d}$ females treated with saline or LIF. Number within the bar indicates the number of mice with implantation sites per total tested mice.

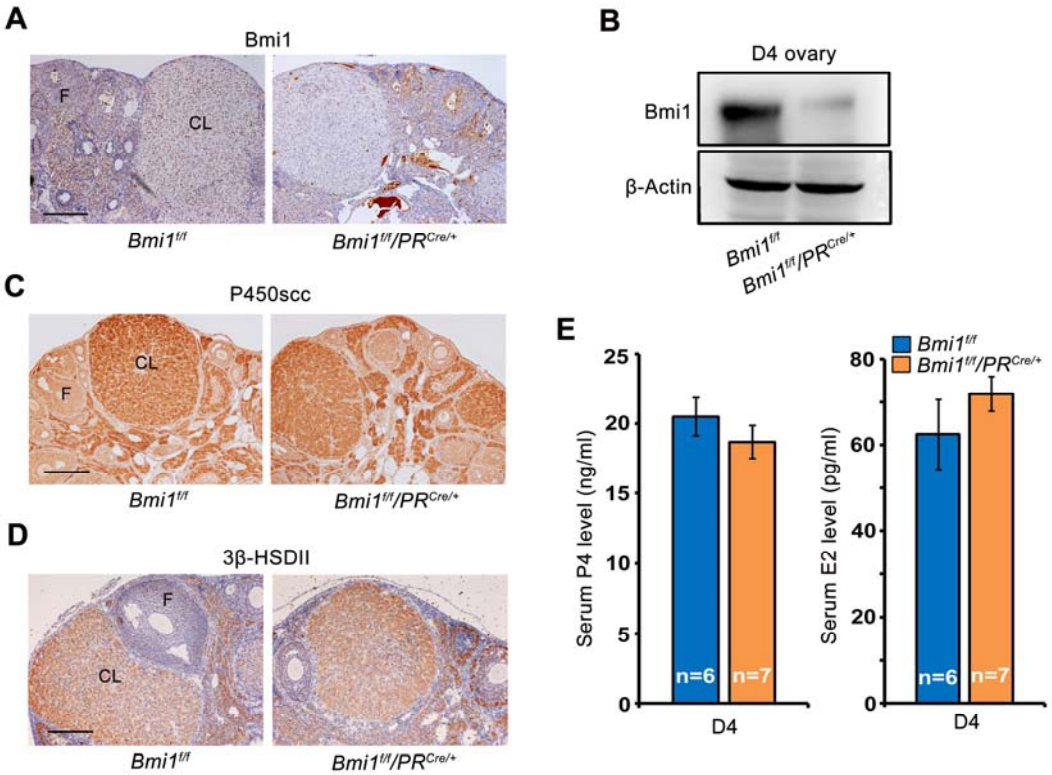

Supplementary Figure 3: Apparently normal ovarian steroid hormone secretion at periimplantation in *Bmi1$^{d/d}$* females

(**A**, **B**) Immunohistochemistry and Immunoblotting analysis of Bmi1 protein in *Bmi1$^{f/f}$* and *Bmi1$^{d/d}$* ovaries. CL, corpus luteum; F, follicle. Scale bars, 100 µm. β-Actin serves as a loading control. (**C**, **D**) Immunostaining of P450scc and 3β-HSDII in day 4 *Bmi1$^{f/f}$* and *Bmi1$^{d/d}$* ovaries. CL, corpus luteum; F, follicle. Scale bars, 100 µm. (**E**) Comparable serum levels of E2 and P4 in day 4 *Bmi1$^{f/f}$* and *Bmi1$^{d/d}$* mice. Number within the bar indicates the number of mice tested. Data represent mean ± SEM, independent-samples Student t-Test.

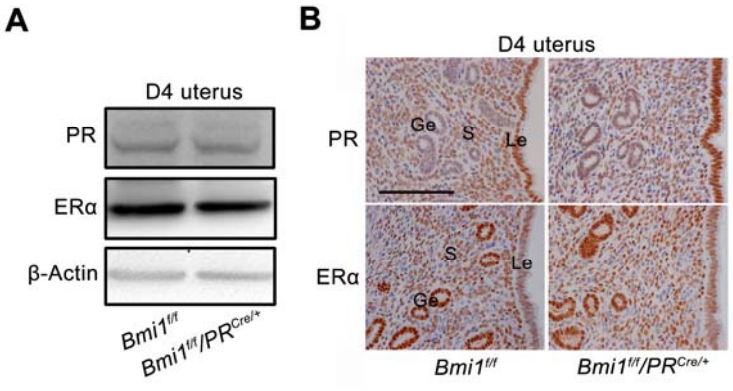

Supplementary Figure 4: *Bmi1*$^{f/f}$ and *Bmi1*$^{d/d}$ mice exhibit comparable expression levels of PR and ERα in day 4 uteri

(**A**, **B**) Immunoblotting and immunostaining analysis reveals normal expression profiles of ERα and PR in *Bmi1*$^{f/f}$ and *Bmi1*$^{d/d}$ uteri on day 4 of pregnancy. β-Actin serves as a loading control. Black scale bar, 100 μm. Le, luminal epithelium; S, stroma; Ge, glandular epithelium.

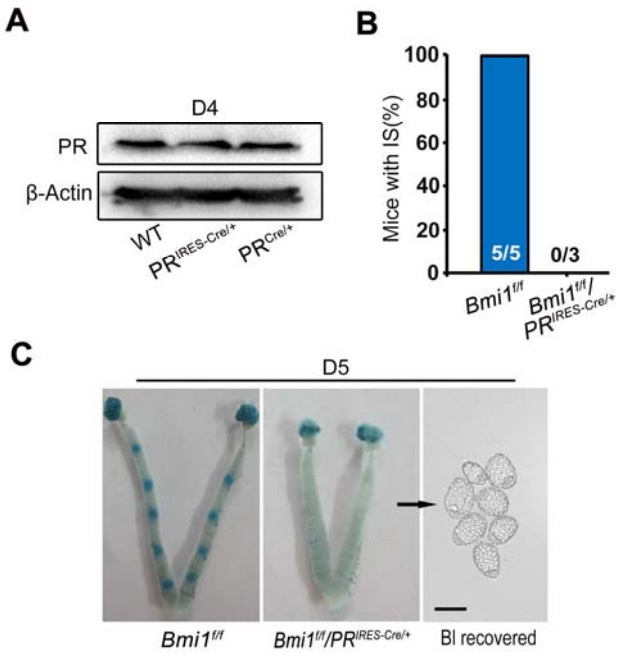

Supplementary Figure 5: Uterine-selective depletion of Bmi1 using $PR^{IRES-Cre/+}$ mouse model results in embryo implantation failure

(**A**) Immunoblotting analysis indicates a comparable expression level of PR protein in day 4 *WT*, $PR^{IRES-Cre/+}$ and $PR^{Cre/+}$ uteri. β-Actin serves as a loading control. (**B-C**) Implantation rate and representative morphology of uteri from $Bmi1^{f/f}$, $Bmi1^{f/f}/PR^{IRES-Cre/+}$ females on day 5 of pregnancy. Embryos recovered from $Bmi1^{f/f}/PR^{IRES-Cre/+}$ uteri without signs of blue reaction. Number within the bar indicates the number of mice with implantation sites per total tested mice. Bl, blastocyst.

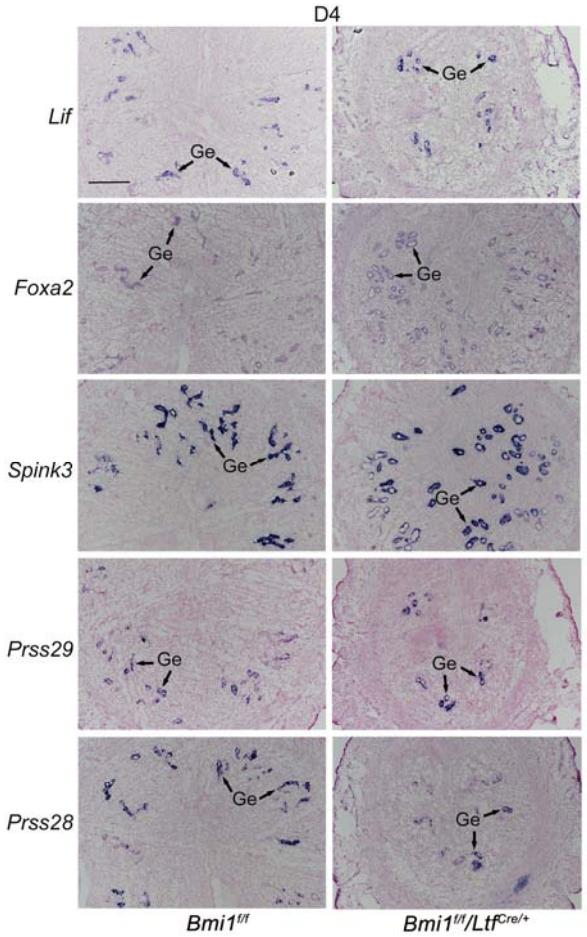

Supplementary Figure 6: Epithelial-selective depletion of Bmi1 didn't affect the glandular epithelium differentiation

In situ hybridization with the DIG-labeled probe analysis the gland-specific genes in *Bmi1*$^{f/f}$, *Bmi1*$^{f/f}$/*Ltf*$^{Cre/+}$ mice. Ge, glandular epithelium. Black scale bar, 100 μm.

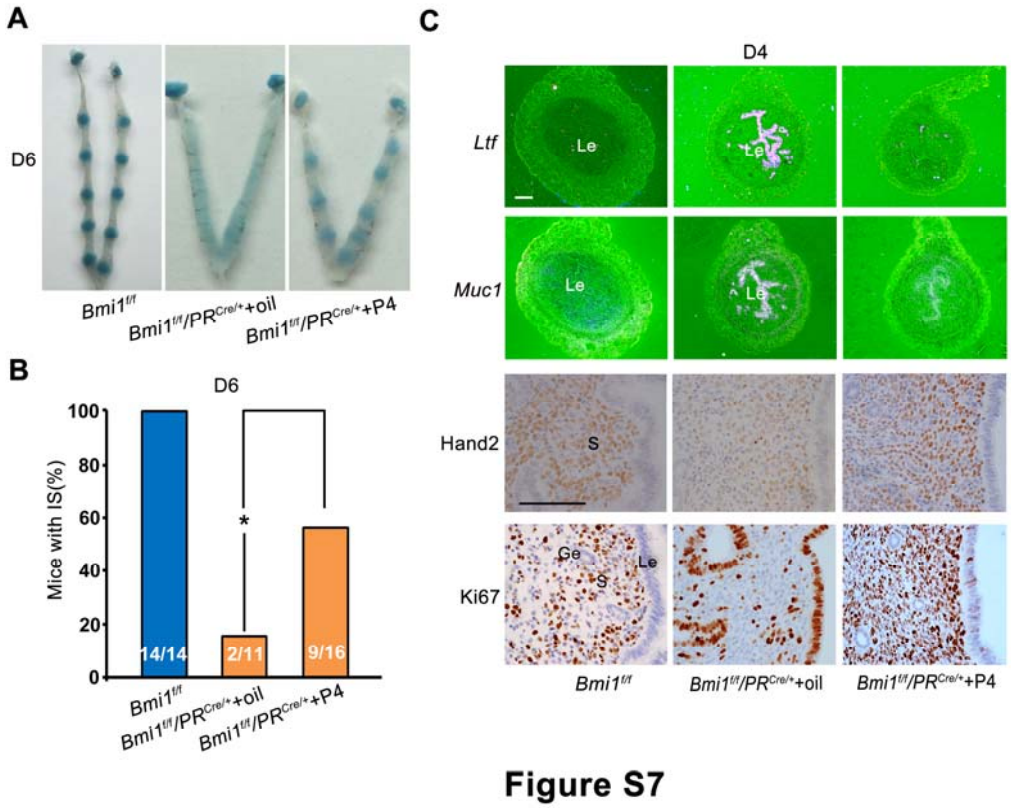

Figure S7

Supplementary Figure 7: Exogenous P4 supplementation can partially improve implantation rate in *Bmi1* mutant females

(**A**, **B**) Implantation rate and representative uteri from *Bmi1*$^{f/f}$, *Bmi1*$^{d/d}$ females treated with oil or P4 when analyzed on day 6 of pregnancy. Number within the bar indicates the number of mice tested. (**C**) *In situ* hybridization and immunostaining analysis of receptivity marker genes in *Bmi1*$^{f/f}$, *Bmi1*$^{d/d}$ mice receiving oil versus P4 treatment. White scale bar, 100 µm; Black scale bar, 100 µm. Le, luminal epithelium; S, stroma, Ge, glandular epithelium. Data represent mean ± SEM (n=3; *P < 0.05), independent-samples Student t-Test.

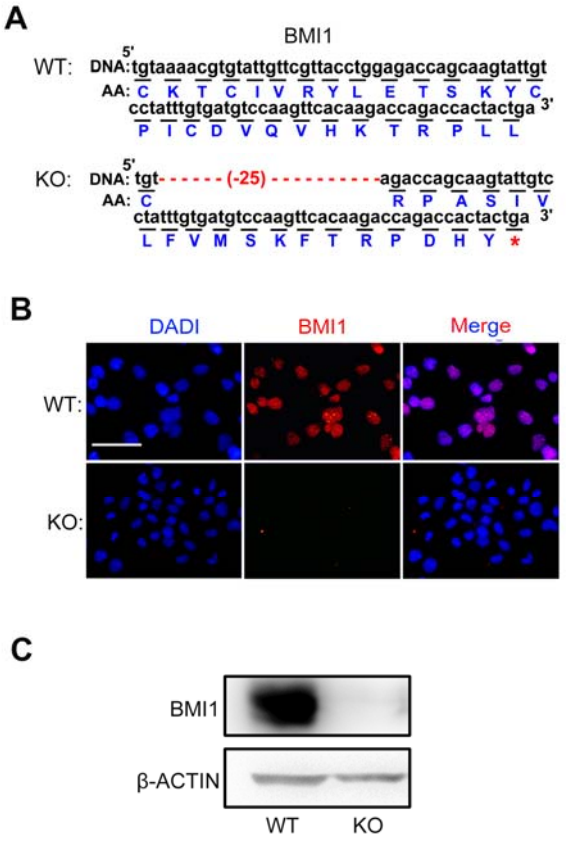

Supplementary Figure 8: BMI1 knockout human Ishikawa cell line is generated via employing CRISPR/Cas9 strategy

(**A**) Information of BMI1 knockout cell line. Twenty-five bases of nucleic acids are deleted at coding sequence resulting in frameshift mutation and the translation termination by a stop codon soon after the mutant site. DNA, DNA sequence; AA, amino acid sequence. (**B**, **C**) Immunoblotting and immunofluorescence staining analysis reveals a complete deletion of BMI1 proteins in null mutant Ishikawa cells. β-ACTIN serves as a loading control. Scale bars, 100 μm.

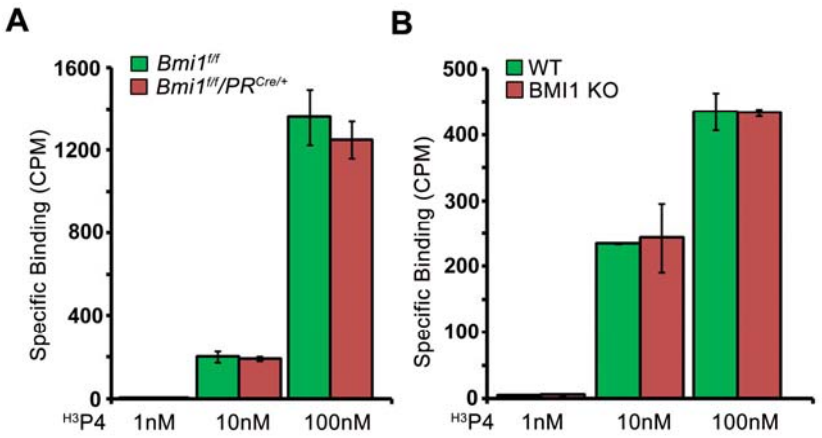

Supplementary Figure 9: PR ligand-receptor binding activity is comparable in *Bmi1*$^{f/f}$ versus *Bmi1*$^{d/d}$ mice as well as in the wild-type (WT) versus BMI1 KO Ishikawa cells

(**A**, **B**) Ligand-receptor binding assay using radiolabeled $^{[3H]}$P4 reveals a normal P4-PR binding affinity both in *Bmi1*$^{d/d}$ uteri and null mutant Ishikawa cells. A competition hormone binding assay is performed using 1, 10, 100 nM of $^{[3H]}$P4 and increasing amounts of unlabeled P4. Data represent mean ± SEM (n=3), independent-samples Student t-Test.

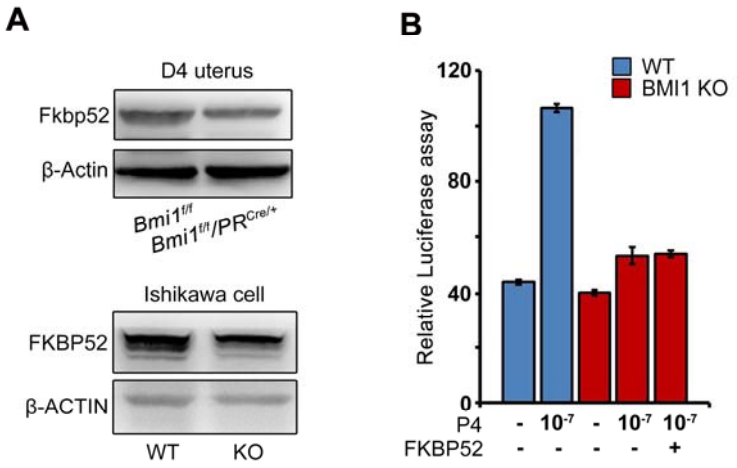

Supplementary Figure 10: Downregulated FKBP52 expression is not the cause for impaired PR responsiveness upon loss of BMI1

(**A**) Immunoblotting analysis shows a significantly downregulated Fkbp52 expression in both *Bmi1*$^{d/d}$ uteri and BMI1 KO Ishikawa cells. β-Actin serves as a loading control. (**B**) Co-transfection of FKBP52 fails to restore PR sensitivity in BMI1 KO Ishikawa cells. Data represent mean ± SEM (n=3), independent-samples Student t-Test.

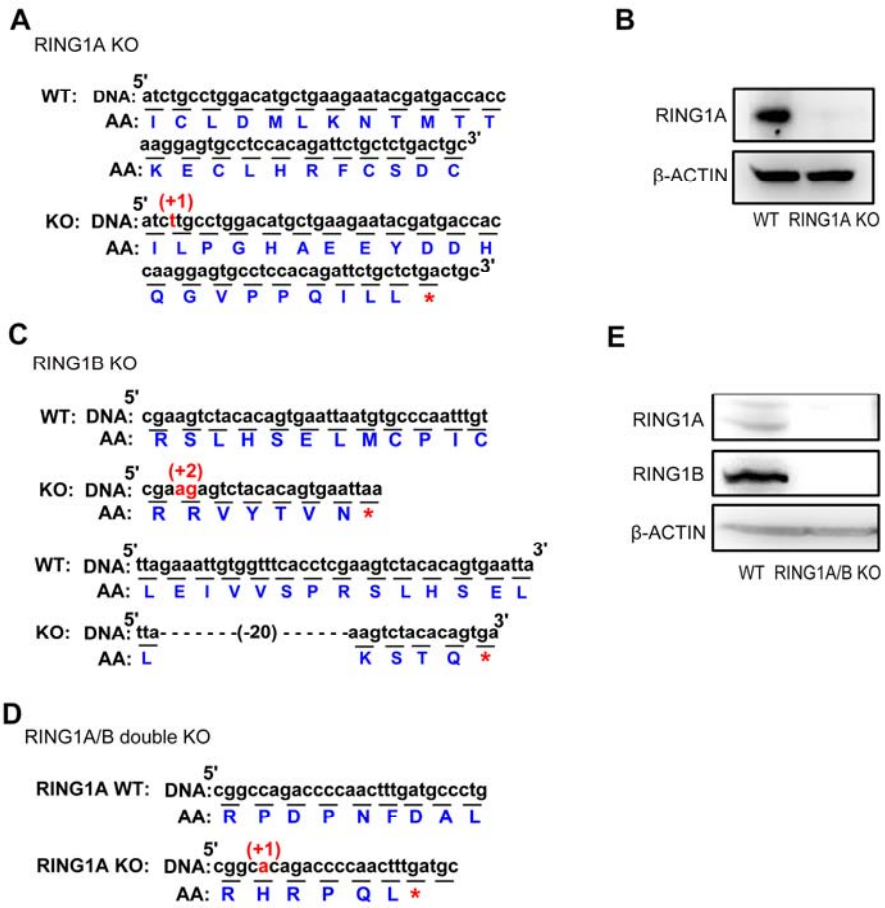

Supplementary Figure 11: Ring1A KO, Ring1B KO, and Ring1A/B double KO Ishikawa cell lines are established by CRISPR/Cas9 strategy

(**A**) Information of RING1A knockout cell line. A base of nucleic acid is added at coding sequence resulting in frameshift mutation and the translation termination by a stop codon soon after the mutant site. DNA, DNA sequence; AA, amino acid sequence. (**B**) Immunoblotting analysis exhibits a complete deletion of RING1A protein in null mutant cells. β-ACTIN serves as a loading control. (**C**) Information of RING1B knockout cell line. In two alleles, twenty bases of nucleic acids are deleted and two bases of nucleic acids are added respectively at coding sequence resulting in frameshift mutation and the translation termination by a stop codon soon after the mutant site. (**D**) Information of RING1A/B double knockout cell line. In above-mentioned RING1B knockout Ishikawa cell line, a base of nucleic acid is added at RING1A coding sequence resulting in frameshift mutation and the translation termination by a stop codon soon after the mutant site. (**E**) Immunoblotting analysis reveals a complete deletion of RING1A and RING1B proteins in double mutant Ishikawa cells. β-ACTIN serves as a loading control.

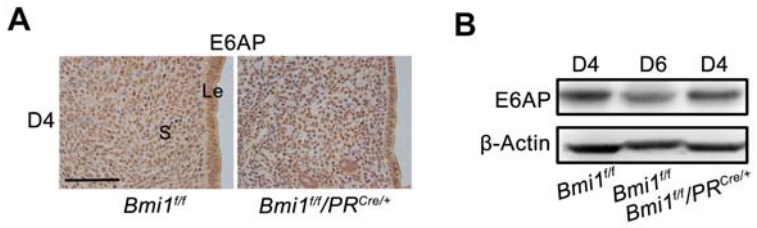

Supplementary Figure 12: E6AP is normally expressed in *Bmi1*$^{f/f}$ and *Bmi1*$^{d/d}$ mouse uteri

(**A**, **B**) Immunohistochemical staining and immunoblotting analysis indicate a comparable expression level of E6AP in day 4 *Bmi1*$^{f/f}$ and *Bmi1*$^{d/d}$ uteri. Black scale bar, 100µm. β-Actin serves as a loading control.

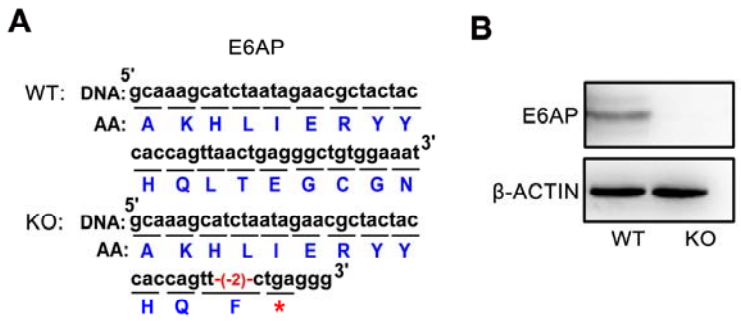

Supplementary Figure 13: E6AP knockout human Ishikawa cell line is established by CRISPR/Cas9 strategy

(**A**) Information of E6AP knockout cell line. Two bases of nucleic acids are deleted at coding sequence resulting in frameshift mutation and the translation termination by a stop codon soon after the mutant site. DNA, DNA sequence; AA, amino acid sequence. (**B**) Immunoblotting analysis shows a complete deletion of E6AP proteins in null mutant Ishikawa cells. β-ACTIN serves as a loading control.

Supplementary Table 1: Antibody information

Antibodies	Company	Catalog/clone Number	Dilution	Application
Bmi1	Abcam	Ab14389	1:200	Immunohistochemistry
Ki67	Epitomics	4203-1	1:500	Immunohistochemistry
ERα	Dako	M7047	1:200	Immunohistochemistry
PR	Dako	A0098	1:100	Immunohistochemistry
P450-scc	Santa Cruz	Sc-18043	1:100	Immunohistochemistry
E6AP	Thermo	PE204355	1:200	Immunohistochemistry
3β-HSD	Santa Cruz	Sc-30820	1:100	Immunohistochemistry
Hand2	Santa Cruz	Sc-9409	1:200	Immunohistochemistry
BrdU	Abcam	Ab6326	1:500	Immunohistochemistry
HA	ABclone	AE008	1:200	Immunohistochemistry
Flag	Sigma	F1804	1:200	Immunohistochemistry
Cox2	CST	D5H5	1:200	Immunohistochemistry
β-Actin	Sigma	A4700	1:5000	Immunoblot
Fkbp52	Abcam	Ab129097	1:1000	Immunoblot
ERα	Santa Cruz	Sc-542	1:1000	Immunoblot
Bmi1	Abcam	Ab14389	1:1000	Immunoblot/IP
E6AP	Thermo	PE204355	1:1000	Immunoblot
RING1B	Abcam	Ab28629	1:1000	Immunoblot
HA	ABclone	AE008	1:5000	Immunoblot/IP
Flag	Sigma	F1804	1:5000	Immunoblot/IP
RING1A	Santa Cruz	Sc-28736	1:1000	Immunoblot
Myc	ABclone	AE018	1:2000	Immunoblot/IP
Ubiquitin	Abcam	Ab8920	1:1000	Immunoblot
His	ABclone	AE523	1:1000	Immunoblot/IP
H2AK119Ub	Millipore	E6C5	1:1000	Immunoblot
PR	CST	C89F7	1:1000	Immunoblot/IP

Supplementary Table 2: Primers for Real-time PCR

Genes	Primers
PGR-Homo-F	5'-TGGACAAGGAGACAAGTAAT-3'
PGR-Homo-R	5'-TTAGTGAAGTAAGGATAAGCA-3'
GAPDH-Homo-F	5'-GTCGCCAGCCGAGCCACATC-3'
GAPDH-Homo-R	5'-CCAGGCGCCCAATACGACCA-3'
BMI1-Homo-F	5'-CGAACAACGAGAATCAAGAT-3'
BMI1-Homo-R	5'-CCAGGTAACGAACAATACAC-3'
TGFB1-Homo-F	5'-AACCCACAACGAAATCTATG-3'
TGFB1- Homo -R	5'-CCAGGAATTGTTGCTGTATT-3'
NPAS2-Homo-F	5'-AATTCACTTCAAGGCATAGC-3'
NPAS2-Homo-R	5'-TCATCAATGTGGTAGTAGTCA-3'
E6AP-Homo-F	5'-TGCCATTGTTGCTGCTTCGA-3'
E6AP-Homo-R	5'-TGGACTCAGGGATGGGCTCT-3'
FOSL2-Homo-F	5'-GCGGATCATGTACCAGGATTAT-3'
FOSL2-Homo-R	5'-CAGGCATATCTACCCGGAATTT-3'
JUN-Homo-F	5'-TCCAAGTGCCGAAAAAGGAAG-3'
JUN-Homo-R	5'-CGAGTTCTGAGCTTTCAAGGT-3'
IRS-Homo-F	5'-CCTCACGTCGATGGCGATGTAGT-3'
IRS-Homo-R	5'-GGGCTTGGTCGGTTGTCCTGG
Hsd11b2-Mus-F	5'-ACCCCTGCTTGGCAGCCTACGG-3'
Hsd11b2-Mus-R	5'-TCACATTAGTCACTGCCTCTGTC-3'
Lif-Mus-F	5'-TCTATGGTTCCAGGCCTTTCC-3'
Lif-Mus-R	5'-CTATGGTTCCAGGCCTTTCCTAA-3'
Hand2-Mus-F	5'-TCGGTTATCTAGTGCTGTC-3'
Hand2-Mus-R	5'-ATACTTACAATGTTTACACCTTCA-3'
Muc1-Mus-F	5'-AGCCCCTATGAGGAGGTTTCG-3'
Muc1-Mus-R	5'-AAGTGGTCACCACAGCTGGG-3'
Ltf-Mus-F	5'-GGGCAAGTGCGGTTTAGTT-3'
Ltf-Mus-R	5'-CCATTGCTTTGGAGGATTT-3'
Areg-Mus-F	5'-GACAAGAAAATGGGACTGTGC-3'
Areg-Mus-R	5'-GGCTTGGCAATGATTCAACT-3'
Gapdh-Mus-F	5'-TGGCAAAGTGGAGATTGTTGCC-3'

Gapdh-Mus-R	5'-AAGATGGTGATGGGCTTCCCG-3'
Bmi1-Mus-F	5'-CGCTCTTTCCGGGATCTTTT-3'
Bmi1-Mus-R	5'-CCCTCCACACAGGACACACAT-3'
Hoxa10-Mus-F	5'-GGCAGTTCCAAAGGCGAAAA-3'
Hoxa10-Mus-R	5'-CAAAAAAAGCCAGAACAAAC-3'
Ihh-Mus-F	5'-CATCTTCAAGGACGAGGAGAACA-3'
Ihh-Mus-R	5'-CATGACAGAGATGGCCAGTGA-3'
Igf1-Mus-F	5'-CTTGAAGATAAAGATACACATCA-3'
Igf1-Mus-R	5'-TGGGCTTGTTGAAGTAAA-3'

Supplementary Table 3: sgRNA sequences

Primer name	Sequences
E6AP-Cas9-Homo-F	5'-CACCGCTACTACCACCAGTTAACTG-3'
E6AP-Cas9-Homo-R	5'-AAACCAGTTAACTGGTGGTAGTAGC-3'
RING1A-Cas9-Homo-F	5'-CACCGACTCATGTGCCCTATCTGCC-3'
RING1A-Cas9-Homo-R	5'-AAACGGCAGATAGGGCACATGAGTC-3'
RING1B-Cas9-Homo-F	5'-CACCGAATTCACTGTGTAGACTTCG-3'
RING1B-Cas9- Homo-R	5'-AAACCGAAGTCTACACAGTGAATTC-3'
BMI1-Cas9-Homo-F	5'-CACCGAACGTGTATTGTTCGTTACC-3'
BMI1-Cas9-Homo-R	5'-AAACGGTAACGAACAATACACGTTC-3'

Supplementary Table 4: Clinical parameters of spontaneous miscarriage patients undertaken IVF treatment

Patients No.	1	2	3	4	5	6	7	8	9	10	11	12	13	14	15	16
Age (years)	26	37	40	27	27	33	25	30	32	42	38	38	26	28	29	28
BMI (kg/m^2)	21.09	31.23	25.00	20.23	19.23	22.86	21.30	21.97	27.55	24.03	26.04	26.35	28.08	22.60	22.43	32.69
Menstrual cycle (days)	60-90	30	26-28	28	28	28-30	25-30	30	28-30	28-32	17-60	28-32	28-30	24-26	28-32	28-30
Basal FSH (IU/L)	4.31	4.67	8.48	4.13	6.94	4.99	6.36	6.08	6.31	5.80	4.19	5.45	6.00	9.20	6.77	6.77
Basal LH (IU/L)	5.69	8.24	6.98	4.09	9.62	4.68	4.76	3.69	7.45	4.61	4.02	4.89	4.35	5.63	6.11	2.97
Basal E2 (pg/ml)	26.40	44.00	23.10	30.70	42.90	37.00	27.20	27.70	43.80	26.50	152.7	39.40	25.80	75.40	33.80	23.70
Basal P4 (ng/ml)	1.27	1.17	0.86	0.59	0.61	0.81	0.52	0.67	0.99	0.96	1.17	0.79	0.42	0.50	0.71	0.54
Basal PRL (ng/ml)	22.88	9.33	8.09	14.20	20.94	19.76	21.73	11.97	15.94	18.58	19.76	10.90	14.89	16.68	18.93	13.28
Basal T (ng/dl)	37.99	40.70	11.07	12.45	36.12	39.95	10.48	19.79	33.45	23.63	27.35	30.90	26.80	18.69	36.91	43.28
TSH (µIU/ml)	4.840	2.560	3.100	2.210	3.720	0.965	2.690	1.590	2.690	3.430	4.160	1.840	2.280	4.000	1.190	3.430
Embryo transfer No.	1	1	2	1	1	2	1	1	1	2	1	2	1		1	1
Embryonic type	Bl	Bl	8-Cell	Bl	Bl	8-Cell	Bl	Bl	Bl	8-Cell	Bl	8-Cell	Bl	8-Cell	Bl	8-Cell
Pretransfer endometrial thickness (cm)	0.90	0.90	1.25	1.00	1.30	0.90	0.90	1.10	0.95	1.30	0.85	1.00	1.10	1.00	0.80	1.00
Abortion weeks+days	8+5	8+1	8+3	8+6	8+3	8+3	8+6	9+2	8+3	8+5	8+1	8+6	9+5	8+6	8+3	8+4
EVCA	Normal	Normal	Normal	Normal	Normal	Normal	Normal	Normal	Normal	Normal	Normal	Normal	Normal	Normal	Normal	Normal

Embryonic Villi Chromosome Analysis, EVCA; Thyroid stimulating hormone, TSH; Testosterone, T; Prolactin, PRL; Luteinizing Hormone, LH; Follicle-stimulating hormone, FSH; Blastocyst, Bl.

Supplementary Table 5: Clinical parameters of successful pregnancy and recurrent implantation failure patients undertaken IVF treatment

Patients No.	1	2	3	1'	2'	3'	4'	5'	6'	7'	8'	9'	10'	11'
Age (years)	31	28	37	38	45	41	30	38	33	28	31	36	34	34
BMI (kg/m^2)	20.76	23.66	25.10	22.03	29.32	23.83	24.44	21.87	17.75	23.71	20.48	21.64	18.33	26.79
Basal FSH (IU/L)	6.38	6.13	9.14	5.31	10.71	6.12	4.72	5.69	5.35	7.29	5.68	8.58	5.61	7.06
Basal E2 (pg/ml)	27.40	25.60	27.30	42.70	31.60	51.50	35.90	40.00	39.80	20.10	21.00	42.40	238.30	36.60
Basal P4 (ng/ml)	0.61	0.24	0.79				0.71	0.46			0.49	0.55	22.29	0.59
Basal LH (IU/L)	5.30	6.45	6.07	3.30	6.83	2.75	2.58	5.51	3.48	5.37	4.82	5.20	3.53	2.70
Basal PRL (ng/ml)	14.51	17.05	10.08	14.41	18.42	22.44	15.85	22.80	33.10	16.23	33.19	18.80	19.76	18.90
Basal T (ng/dl)	30.52	12.66	33.78	41.60	31.00	3.44	27.08	58.38	29.95	22.83	27.54	16.61	16.36	24.81
TSH (µIU/ml)	2.44	1.51	2.31	2.13	2.19	2.19	1.77	1.47	3.20	3.42	2.98	2.98	2.51	1.81
LH (IU/L)	2.27	8.36	6.32	4.66	2.95	8.69	5.80	13.05	4.51	7.88	3.72	11.44	2.33	5.56
E2 (pg/ml)	212.9	171.4	103.8	263.00	198.10	119.80	309.50	354.00	116.40	195.86	173.70	256.10	247.00	259.83
P4 (ng/ml)	11.99	14.04	8.32	7.81	7.28	13.07	14.26	13.71	14.50	13.55	19.47	12.53	15.94	11.95
Pretransfer endometrial thickness (cm)	1.00	1.10	1.20	0.90	0.75	0.70	0.85	0.75	0.90	1.35	0.90	1.00	0.75	0.75
Hysteroscopy	Normal	Normal	Normal	Normal	Normal	Normal	Normal	Normal	Normal	Normal	Normal	Normal	Normal	Normal

Thyroid stimulating hormone, TSH; Testosterone, T; Prolactin, PRL; Luteinizing Hormone, LH; Follicle-stimulating hormone, FSH; Blastocyst, Bl.

Unedited versions of all gel and blot images

Fig 1C

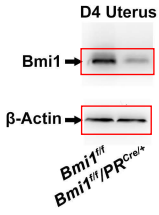

Fig 4D

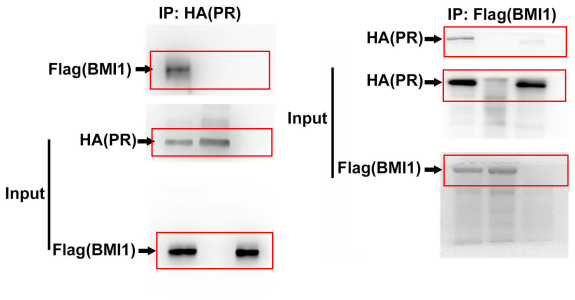

Fig 4E

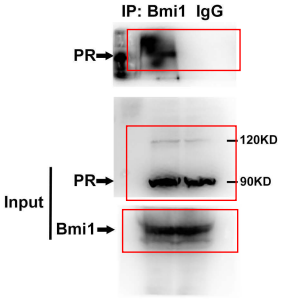

Fig 4I

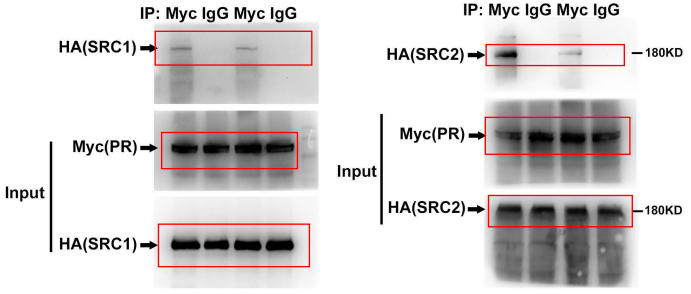

Fig 5A

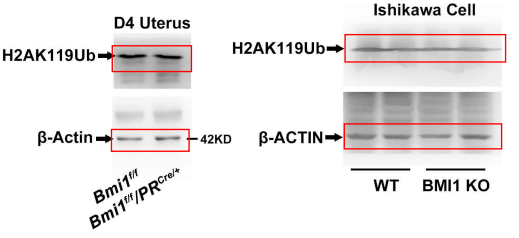

Fig 6A

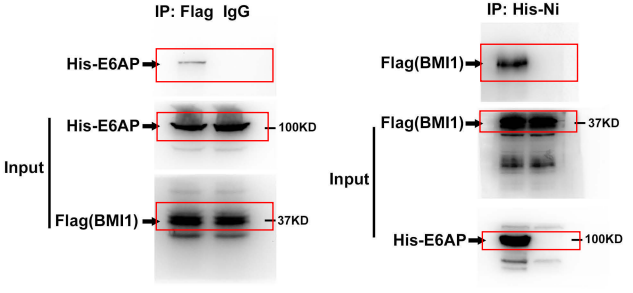

Fig 6B

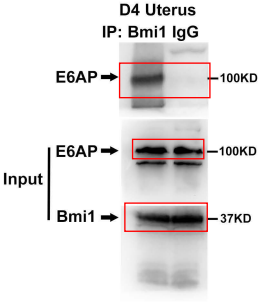

Fig 6H

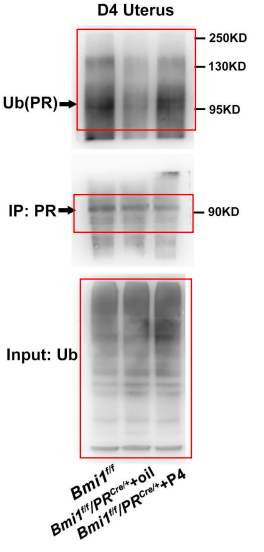

Unedited versions of all gel and blot images

Fig 6G

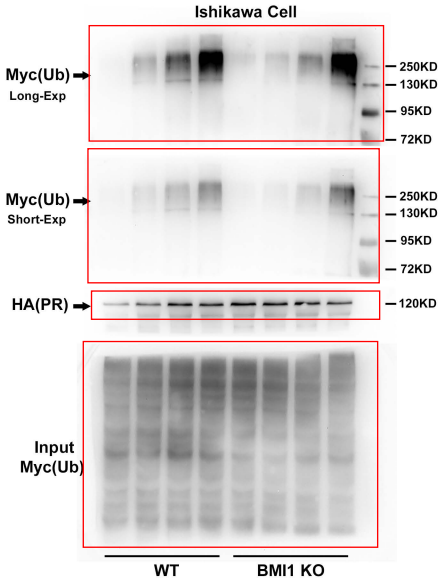

Fig 7B

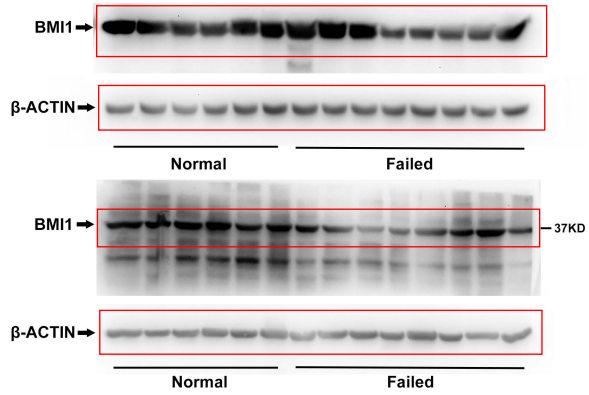

Fig 8A

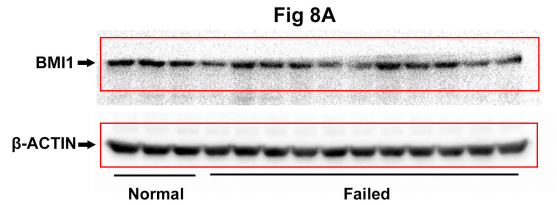

Fig S3B

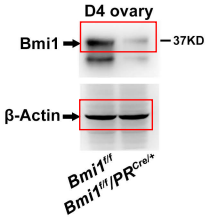

Fig S4A

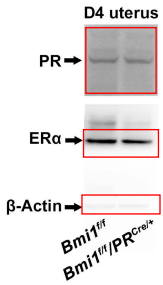

Fig S5A

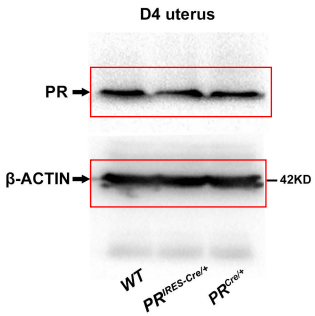

Fig S8C

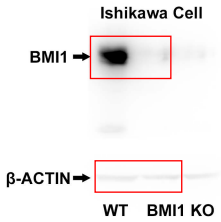

Fig S10A

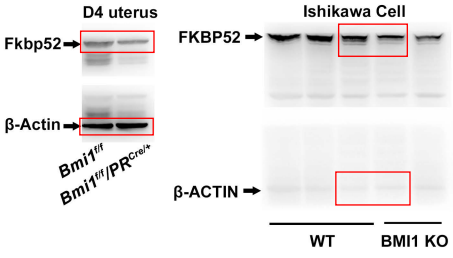

Fig S11B

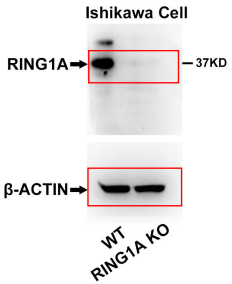

Fig S11E

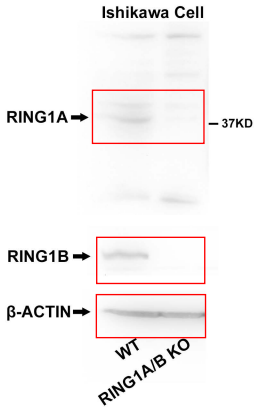

Fig S12B

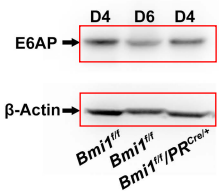

Fig S13B